

Supporting Information

Gate-Opening Gas Adsorption and Host-Guest Interacting Gas Trapping Behavior of Porous Coordination Polymers under Applied AC Electric Fields

Wataru Kosaka, Kayo Yamagishi, Jun Zhang and Hitoshi Miyasaka*

Corresponding author*

Prof. Dr. Hitoshi Miyasaka

Institute for Materials Research, Tohoku University, 2-1-1 Katahira, Aoba-ku, Sendai 980-8577,
Japan

E-mail: miyasaka@imr.tohoku.ac.jp

Tel: +81-22-215-2030

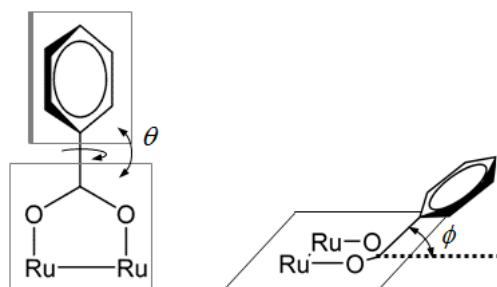
FAX: +81-22-215-2031

Table S1. Crystallographic Data for **3**

	3
formula	C ₄₄ H ₃₆ N ₂ O ₁₂ Ru ₂
formula weight	986.91
crystal system	triclinic
space group	<i>P</i> −1
<i>a</i> / Å	9.461(3)
<i>b</i> / Å	10.660(4)
<i>c</i> / Å	10.261(4)
α / deg	92.650(4)
β / deg	102.491(5)
γ / deg	96.611(5)
<i>V</i> / Å ³	1000.9(6)
<i>Z</i>	1
crystal size / mm ³	0.050×0.010×0.010
<i>T</i> / K	123(1)
<i>D</i> _{calc} / g·cm ^{−3}	1.637
<i>F</i> ₀₀₀	498.00
λ / Å	0.71070
μ (Mo K α) / cm ^{−1}	8.232
data measured	10994
data unique	4474
<i>R</i> _{int}	0.0625
no. of observations	4474
no. of variables	271
<i>R</i> 1 (<i>I</i> > 2.00 σ (<i>I</i>)) ^a	0.0532
<i>R</i> (all reflections) ^a	0.0697
<i>wR</i> 2 (all reflections) ^b	0.1123
GOF	1.092
CCDC No.	1003673

^a $R1 = R = \Sigma ||F_o| - |F_c|| / \Sigma |F_o|$. ^b $wR2 = [\Sigma w(F_o^2 - F_c^2)^2 / \Sigma w(F_o^2)^2]^{1/2}$

Table S2. Selected bond length (Å) and angles (°) for **3**, where θ represents dihedral angle between the least squares planes defined by the phenyl ring of benzoate ligand and a carboxylate-bridging mode (atom set of Ru₂O₂C), and ϕ represents an angle between a carboxylate-bridging plane and C–C bond between phenyl ring and carboxyl carbon.



	1
Ru1–O1	2.049(3)
Ru 1–O2a	2.056(3)
Ru 1–O4	2.051(3)
Ru 1–O5a	2.064(3)
Ru 1–N1	2.402(4)
Ru1–Ru1a	2.2798(9)
Ru1a–Ru1–N1	170.07(8)
θ	
set-1	21.9
set-2	29.5
ϕ	
set-1	3.7
set-2	6.6
Symmetry codes:	(a) $-x+1, -y+1, -z$

On the oxidation state of the [Ru₂] unit in **3.** The oxidation state of [Ru₂] unit can be known from the Ru–O_{eq} length (O_{eq} = equatorial oxygen atoms), which is quite sensitive to the oxidation state of the [Ru₂] unit and to be 2.06–2.07 Å for [Ru₂^{II,II}] and 2.02–2.03 Å for [Ru₂^{II,III}]⁺.¹ The average Ru–O_{eq} length of **1** is 2.055 Å, indicating an oxidation state of [Ru₂^{II,II}].

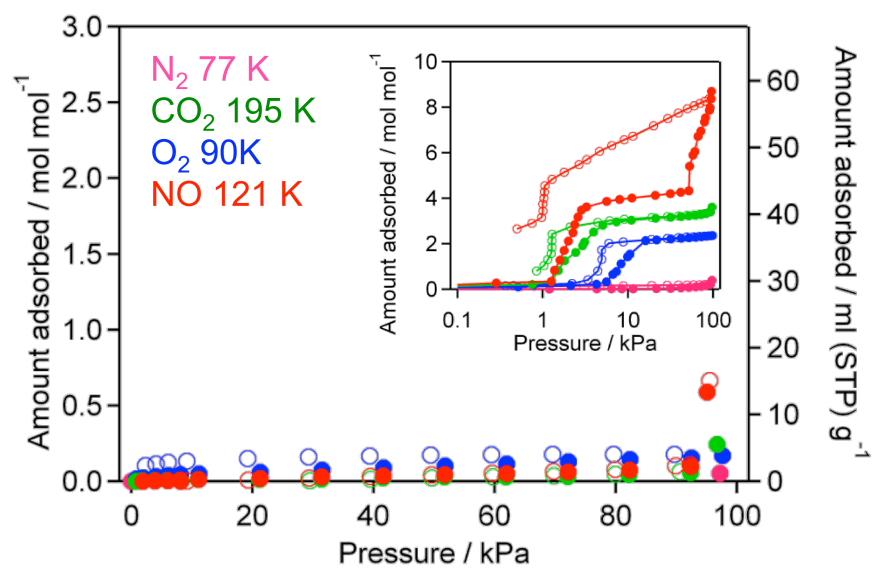


Figure S1. Adsorption (closed circles) and desorption (open circles) isotherms for compound **3** for several gas molecules. Inset: data for compound **1**.

Magnetic properties of 3. The magnetic behavior of **3** is consistent with those for isolated $[\text{Ru}^{\text{II,II}}]$ complexes with an $S = 1$ ground state affected by strong zero-field splitting (ZFS; $D \approx 230 - 320 \text{ cm}^{-1}$) (Figure S2). The χ and χT were simulated using a Curie paramagnetic model with $S = 1$ taking into account zero-field splitting (D), temperature-independent paramagnetism (χ_{TIP}), and impurity with $S = 3/2$ (ρ).² The best fitting parameters were: $g = 2.0$ (fix), $D/k_{\text{B}} = 369(1) \text{ K}$, $\chi_{\text{TIP}} = 66(15) \times 10^{-6} \text{ cm}^3 \text{ mol}^{-1}$, and $\rho = 0.00307(3)$.

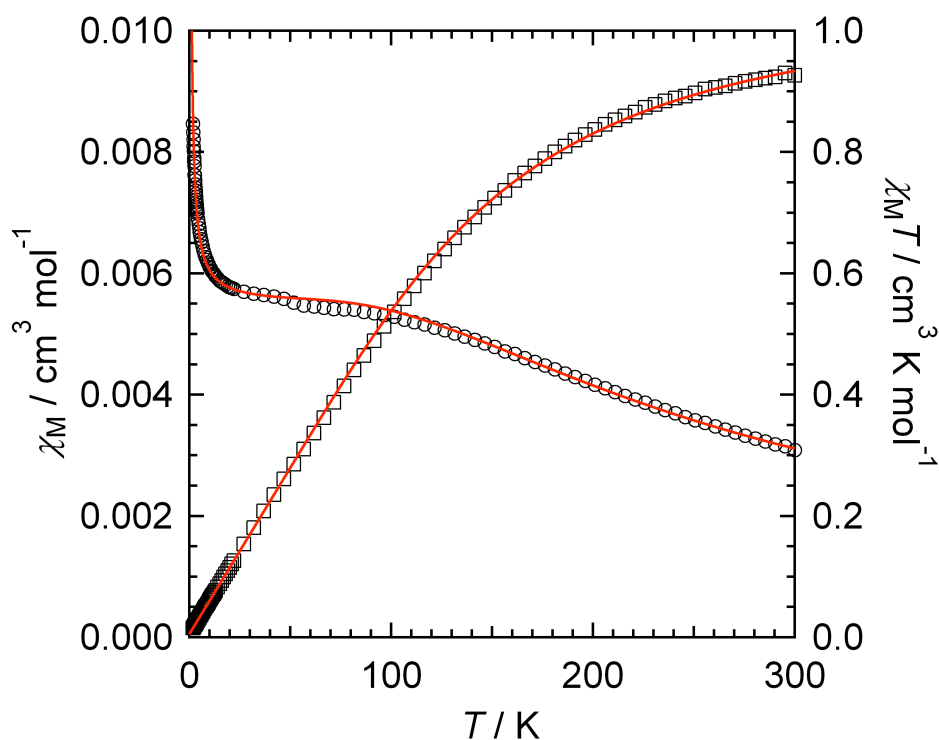


Figure S2. Temperature dependences of χ (\circ) and χT (\square) for **3**, where the red solid lines represent simulated curves based on a Curie paramagnetic model with $S = 1$ taking into account zero-field splitting (D), temperature-independent paramagnetism (χ_{TIP}), and impurity with $S = 3/2$ (ρ)

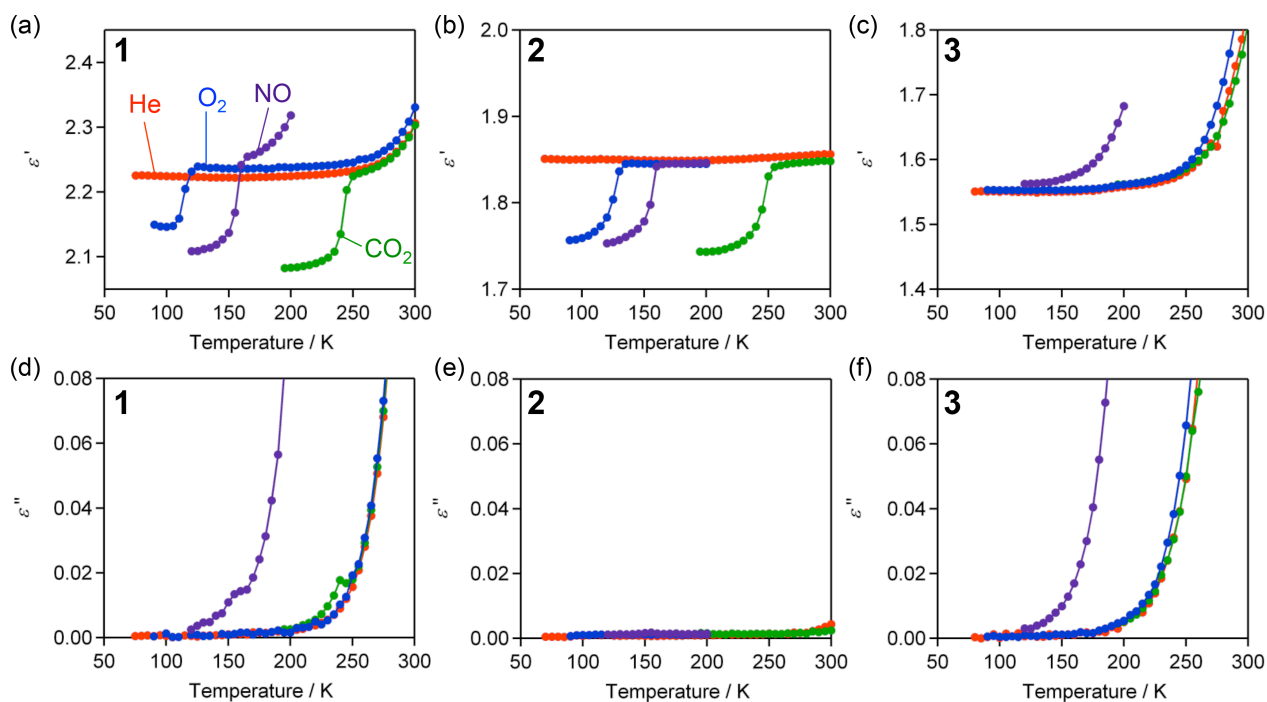


Figure S3. Temperature dependence of the dielectric constant (the real part (ϵ'), (a)–(c); the imaginary part (ϵ''), (d)–(f) for **1** ((a) and (d)), **2** ((b) and (e)), and **3** ((c) and (f)) measured on heating with electric field frequency of 0.1 kHz under 100 KPa of He (red), CO₂ (green), O₂ (blue), and NO (violet).

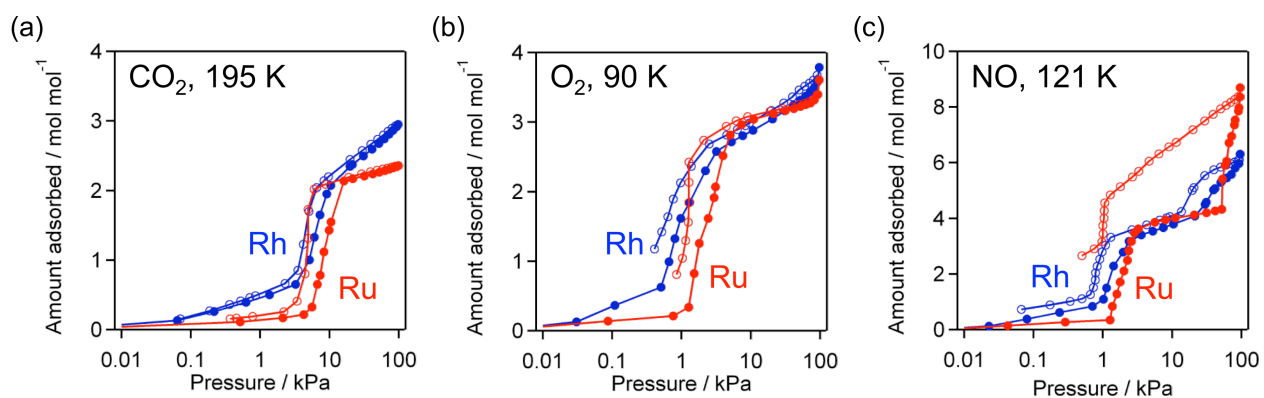


Figure S4. Adsorption isotherms for **1** (red) and **2** (blue); CO_2 at 195 K (a), O_2 at 90 K (b), and NO at 121 K (c). These plots were reproduced from the data reported previously.³

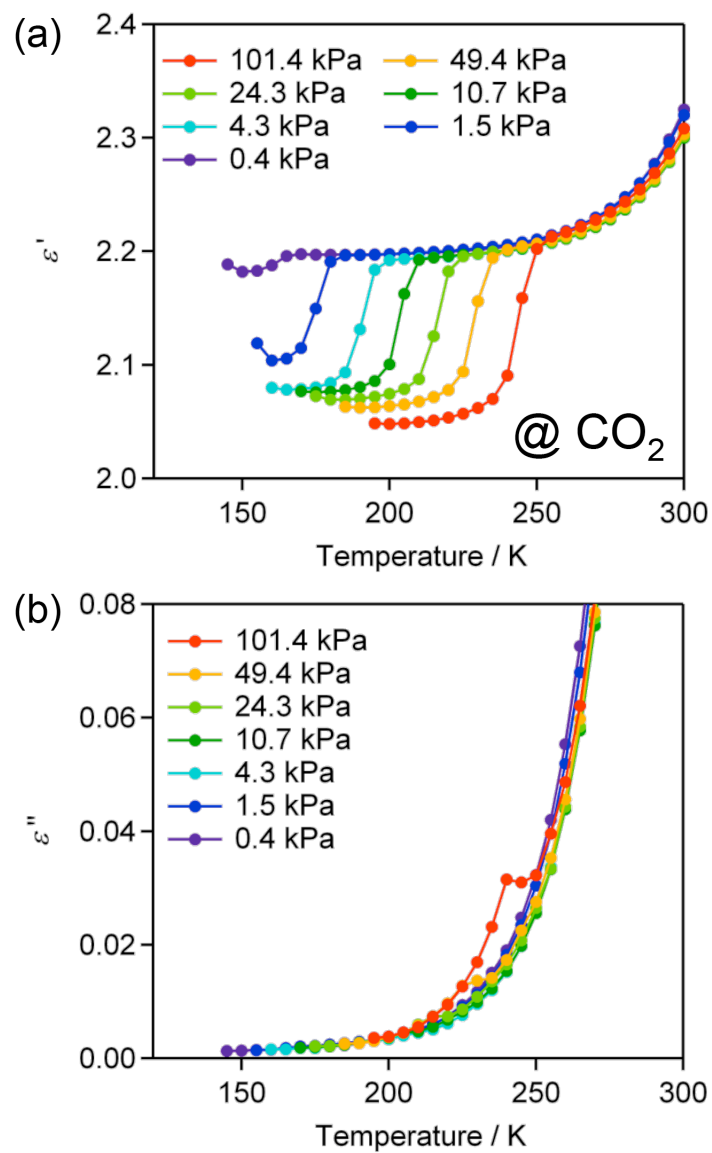


Figure S5. Temperature dependence of the dielectric constants of the real part (ϵ') (a), and the imaginary part (ϵ'') (b) for **1** measured on heating under various pressure of CO₂ with an ac electric field frequency of 0.1 kHz.

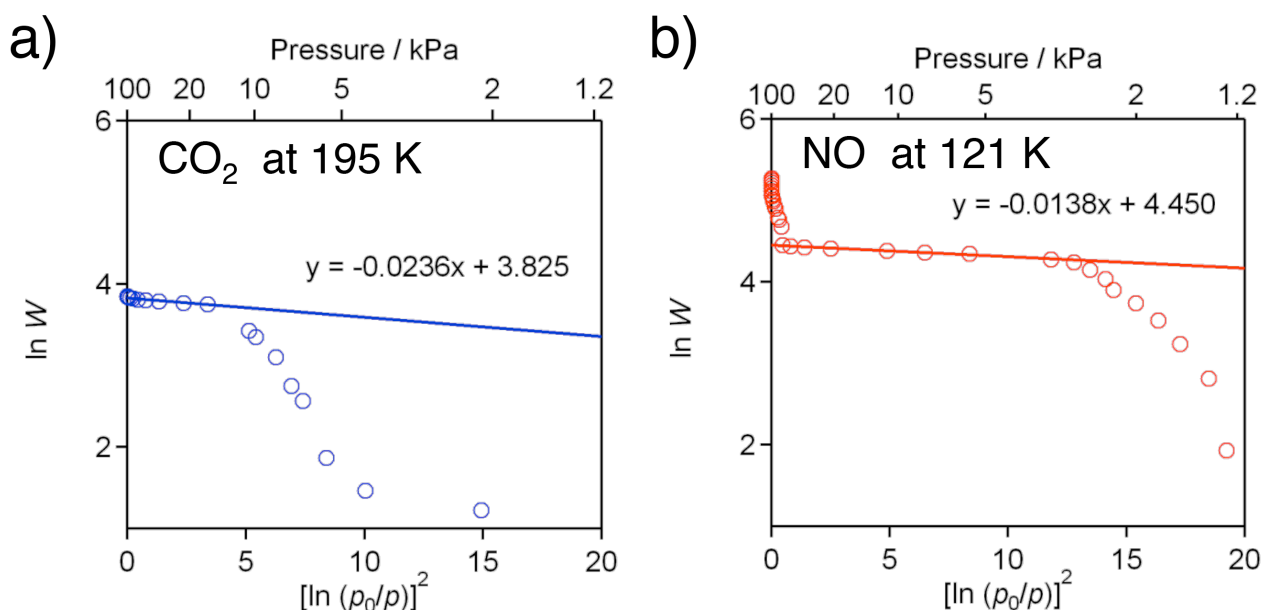


Figure S6. Dubinin-Raduskevich plots on the CO_2 (a) and NO (b) adsorption (195 K for CO_2 and 121 K for NO) for **1**, where the fitting were performed in the range for the diffusional equilibration part from after the 1st gate-opening transition to before the 2nd gate-opening transition. The fitting curves evaluate $\beta E_0 = 10.5 \text{ kJ mol}^{-1}$ for CO_2 and 8.6 kJ mol^{-1} for NO in the DR equation, $\ln W = - (RT/\beta E_0)^2 [\ln(p_0/p)]^2 + \ln W_0$, where β is the affinity coefficient and E_0 is a characteristic adsorption energy.⁴ Note that $q_{\text{st},* = 1/e} = \beta E_0 + \Delta H_v$.

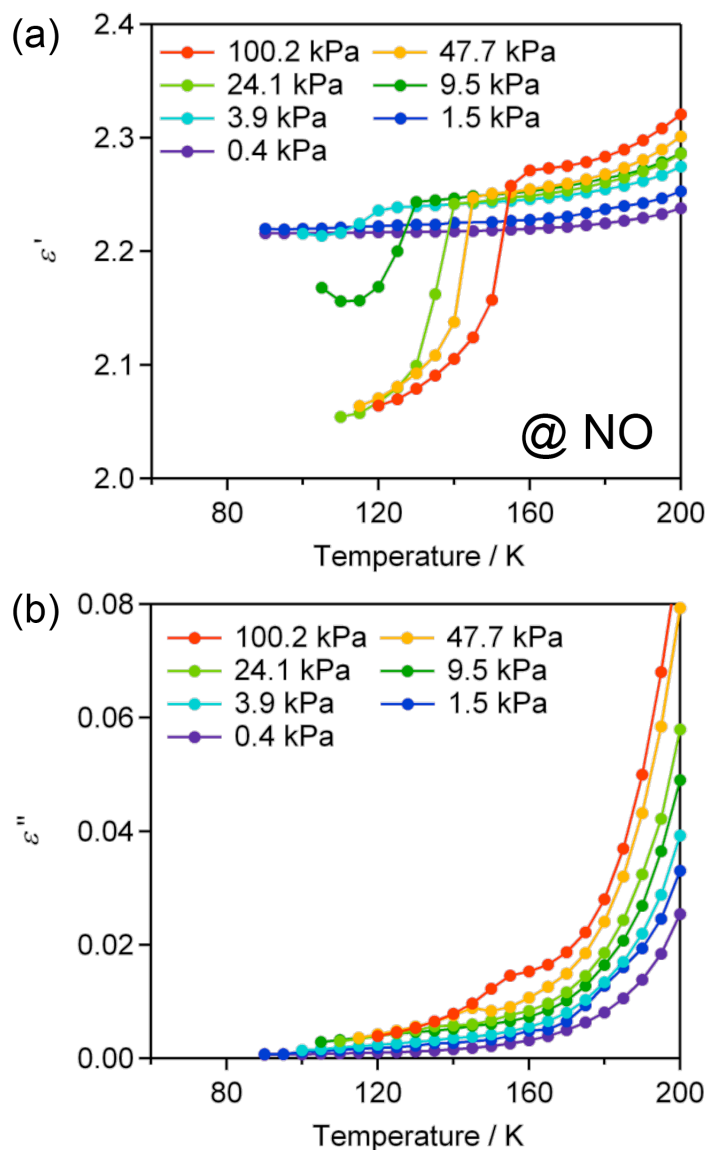


Figure S7. Temperature dependence of the dielectric constants, the real part (ϵ') (a) and the imaginary part (ϵ'') (b), for **1** measured on heating under various pressure of NO with an ac electric field frequency of 0.1 kHz.

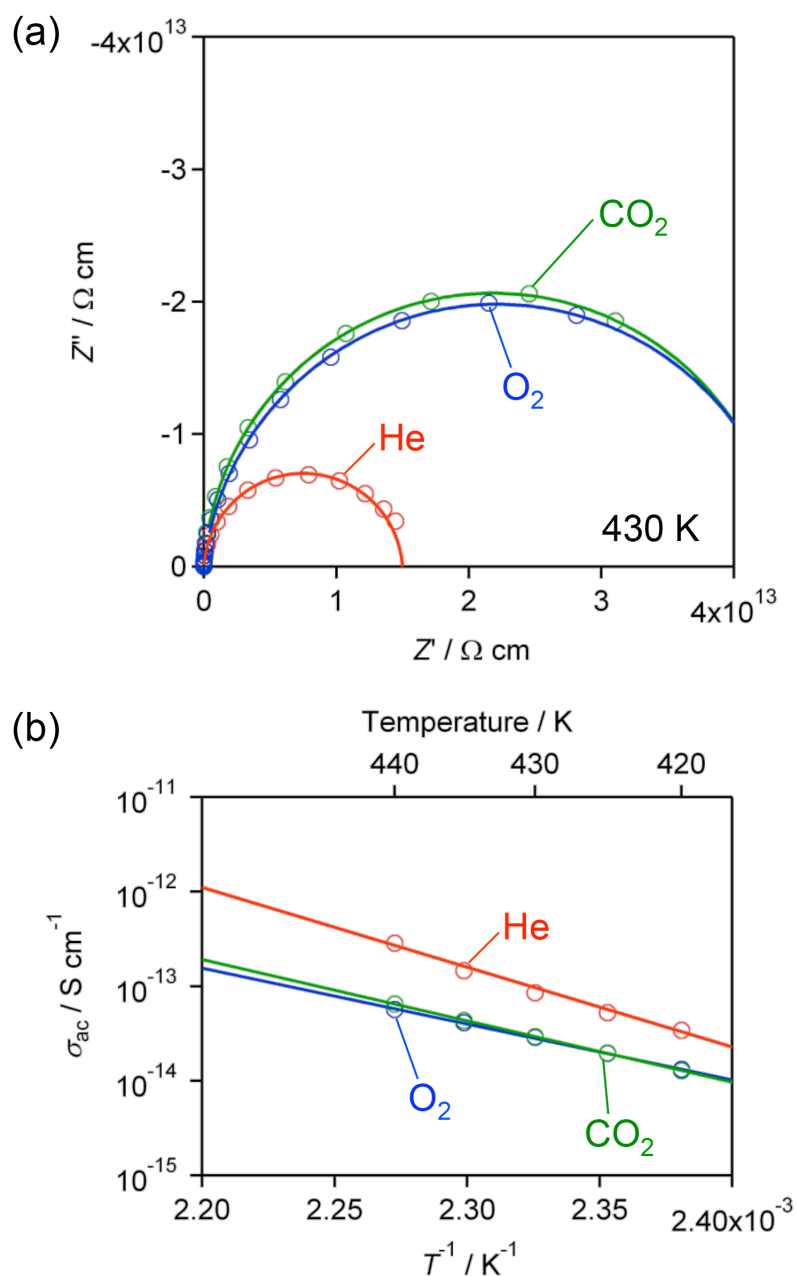


Figure S8. Nyquist plots for **2** at 430 K (a), where the solid lines represent simulation curves based on a generalized Debye equation with a β value in the range of 0.92–0.97, and the Arrhenius plots (b) of σ_{ac} estimated from the Nyquist plots measured at several temperatures under 100 kPa of He (red), CO_2 (green), and O_2 (blue). The activation energy (E_a) is listed in Table 1.

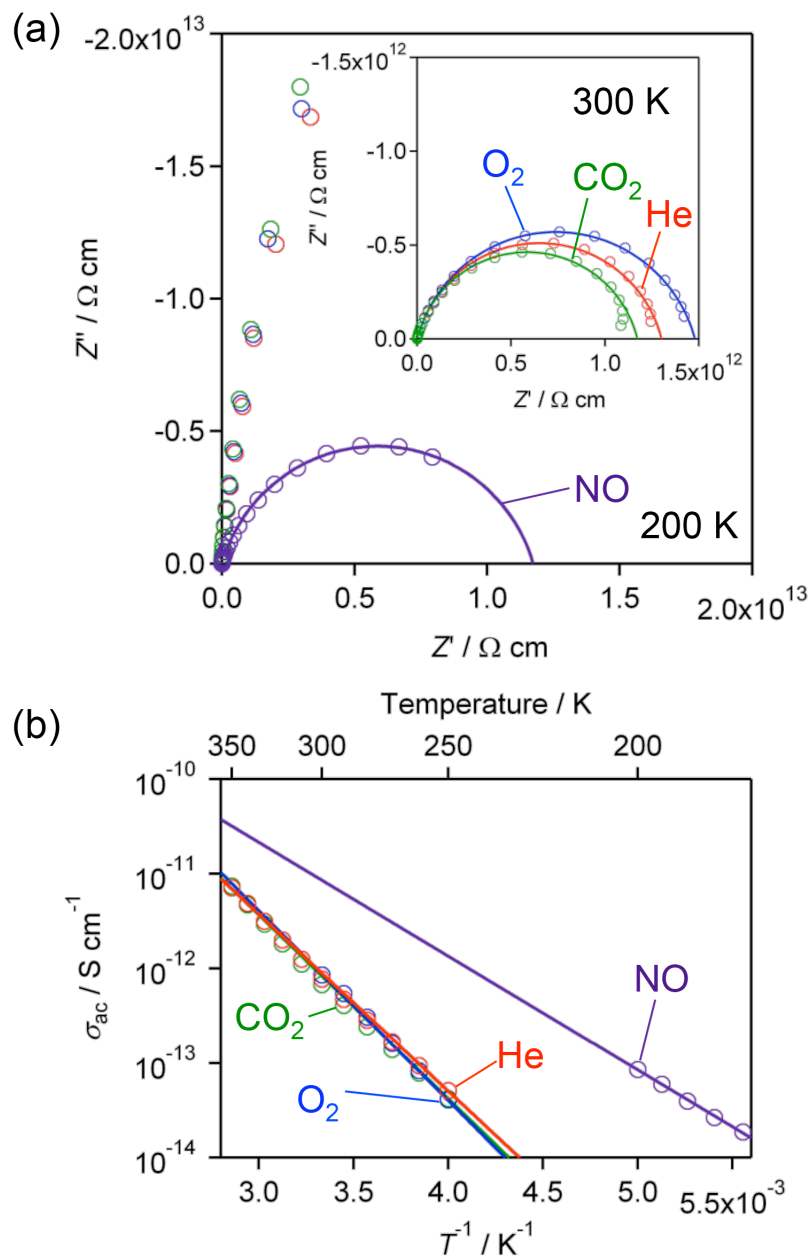


Figure S9. Nyquist plots for **3** at 200 K (a) and 300 K (a, inset), where the solid lines represent simulation curves based on a generalized Debye equation with a β value in the range of 0.78–0.85, and the Arrhenius plots (b) of σ_{ac} estimated from the Nyquist plots measured at several temperatures under 100 kPa of He (red), CO₂ (green), O₂ (blue), and NO (violet). The activation energy (E_a) is listed in Table 1.

References

- (1) Cotton, F. A.; Walton, R. A. *Multiple Bonds Between Metal Atoms*, 2nd ed., Oxford University Press: Oxford, 1993.
- (2) Kahn, O. *Molecular Magnetism*; VCH: New York, 1993.
- (3) Kosaka, W.; Yamagishi, K.; Hori, A.; Sato, H.; Matsuda, R.; Kitagawa, S.; Takata, M.; Miyasaka, H. *J. Am. Chem. Soc.* **2013**, *135*, 18469.
- (4) Matsuda, R.; Kitaura, R.; Kitagawa, S.; Kubota, Y.; Kobayashi, T. C.; Horike, S.; Takata, M. *J. Am. Chem. Soc.* **2004**, *126*, 14063–14070.